THE JOURNAL OF BIOLOGICAL CHEMISTRY
Vol. 277, No. 8, Issue of February 22, pp. 6463–6468, 2002

Printed in U.S.A.

Engineering Photocycle Dynamics

CRYSTAL STRUCTURES AND KINETICS OF THREE PHOTOACTIVE YELLOW PROTEIN HINGE-BENDING MUTANTS*

Received for publication, September 26, 2001, and in revised form, October 29, 2001
Published, JBC Papers in Press, November 19, 2001, DOI 10.1074/jbc.M109313200

Daan M. F. van Aalten‡§¶, Andrea Haker‖, Johnny Hendriks‖, Klaas J. Hellingwerf‖, Leemor Joshua-Tor‡, and Wim Crielaard‖**

From ‡W. M. Keck Structural Biology, Cold Spring Harbor Laboratory, Cold Spring Harbor, New York 11724, §Wellcome Trust Biocentre, Division of Biological Chemistry and Molecular Microbiology, School of Life Sciences, University of Dundee, Dow Street, Dundee DD1 5EH, Scotland, and ‖Swammerdam Institute for Life Sciences, University of Amsterdam, 1018 WV Amsterdam, The Netherlands

Crystallographic and spectroscopic analyses of three hinge-bending mutants of the photoactive yellow protein are described. Previous studies have identified Gly^{47} and Gly^{51} as possible hinge points in the structure of the protein, allowing backbone segments around the chromophore to undergo large concerted motions. We have designed, crystallized, and solved the structures of three mutants: G47S, G51S, and G47S/G51S. The protein dynamics of these mutants are significantly affected. Transitions in the photocycle, measured with laser induced transient absorption spectroscopy, show rates up to 6-fold different from the wild type protein and show an additive effect in the double mutant. Compared with the native structure, no significant conformational differences were observed in the structures of the mutant proteins. We conclude that the structural and dynamic integrity of the region around these mutations is of crucial importance to the photocycle and suggest that the hinge-bending properties of Gly^{51} may also play a role in PAS domain proteins where it is one of the few conserved residues.

The photoactive yellow protein (PYP)[1] is a photoreceptor presumed to be involved in a phototactic response of the bacterium *Ectothiorhodospira halophila* to intense blue light (1). Its structure reveals an α/β fold with the chromophore, *p*-coumaric acid bound to the protein *via* a thioester linkage (2) (see Fig. 1). The protein has been shown to undergo a photocycle, linked to isomerization of the chromophore (3–7). The ground state (pG) has a UV/visible absorbance maximum at 446 nm. After absorption of a blue photon, the protein returns from the primary excited state into the first transient ground-state (8–11), a strongly red-shifted intermediate (12), at the ps time scale. A more moderately red-shifted intermediate (pR), absorbing maximally at 465 nm, is formed on the ns time scale (13). The pR intermediate spontaneously converts into a blue-shifted intermediate (pB; absorbing maximally at 355 nm) at the sub-ms time scale (13, 14). The pB intermediate subsequently relaxes back to pG on a sub-s time scale (10, 13–15) or faster in a light-dependent reaction (16).

Recent Laue diffraction and cryo-crystallographic studies on PYP have given insight into the structural events during and after chromophore isomerization (4, 6, 7). Initially, light absorption induces a flipping of the carbonyl group of the chromophore thioester linkage. At room temperature, in concert with this flipping, the vinyl bond of the chromophore isomerizes from *trans* to *cis*, leading to an ~60 ° rotation of the aromatic ring of the chromophore (4). At low temperature (<150 K), the latter process appears to be blocked about halfway during the isomerization process (7). What both Laue diffraction and cryo-crystallography studies have in common, is that the observed structural changes provide a detailed picture of the early structural events in the photocycle in the immediate environment of the chromophore (4, 6, 7). For PYP in solution, formation of the blue-shifted intermediate pB involves a significant conformational transition, which has the characteristics of a (partial) protein unfolding event, as reported by UV/visible and Fourier transform infrared spectroscopy, mass spectrometry, and ^{1}H-NMR analyses (17–19). These latter observations hint at the presumed signaling function of PYP, which ultimately should result in a negative phototactic response of the bacterium. This presumably happens via a signal transduction pathway, components of which should detect a conformational change in PYP. Thus, in summary, the pG-pR transition in the photocycle represents the structural changes of the chromophore as a result of photon absorption, whereas the pR-pB transition represents the structural adaptation of the protein to the altered conformation of the chromophore.

To study the possible protein motions involved in the photocycle, PYP dynamics have been investigated by computer simulation (20). This study suggested that chromophore-linked, concerted motions may be present in pG and that these motions might be attenuated upon isomerization of the chromophore. The simulations, later supported by x-ray crystallographic

* This research was supported by grants of the Arnold and Mable Beckman Foundation (to L. J.), a European Molecular Biology long-term fellowship (to D. v. A.), and a Wellcome Trust Career Development Research Fellowship (to D. v. A). The costs of publication of this article were defrayed in part by the payment of page charges. This article must therefore be hereby marked "*advertisement*" in accordance with 18 U.S.C. Section 1734 solely to indicate this fact.

The atomic coordinates and structure factors (codes 1GSV for PYP47, 1GSW for PYP57, and 1GSX for PYP47+51) have been deposited in the Protein Data Bank, Research Collaboratory for Structural Bioinformatics, Rutgers University, New Brunswick, NJ (http://www.rcsb.org/)

¶ To whom correspondence may be addressed: Wellcome Trust Biocentre, Div. of Biological Chemistry and Molecular Microbiology, School of Life Sciences, Univ. of Dundee, Dow Street, Dundee DD1 5EH, Scotland. Tel.: 44-1382-344979; Fax: 44-1382-345764; E-mail: dava@davapc1.bioch.dundee.ac.uk.

** To whom correspondence may be addressed: W. M. Keck Structural Biology, 1 Bungtown Rd., Cold Spring Harbor Lab., Cold Spring Harbor, NY 11724. Tel.: 516-367-8821; Fax: 516-367-8873; E-mail: leemor@cshl.org.

[1] The abbreviations used are: PYP, photoactive yellow protein; pG, ground state; pR, red-shifted intermediate; pB, blue-shifted intermediate; MES, 4-morpholineethanesulfonic acid; r.m.s.d., root mean square deviation(s).

TABLE I
Details of data collection and refinement
Values between brackets are for the highest resolution shell.

	PYP47	PYP51	PYP47 + 51
Temperature	100 K	100 K	100 K
Wavelength	1.08 Å	1.08 Å	1.08 Å
Space group	$P6_5$	$P6_5$	$P6_5$
Cell dimensions	a = b = 40.31, c = 116.43 Å	a = b = 36.73, c = 130.19 Å	a = b = 40.42, c = 118.61 Å
Resolution range	15–1.75 Å	15–1.85 Å	20–1.79 Å
Last resolution shell	1.81–1.75 Å	1.92–1.85 Å	1.85–1.79 Å
No. observed refl.	28758	25707	26058
No. unique refl.	10411 (1021)	8430 (829)	9953 (936)
No. test refl.	777	606	736
Redundancy	2.8	3.0	2.6
I/σI	11.6 (2.6)	10.1 (1.9)	9.1 (2.0)
Completeness	96.6% (96.2%)	99.2% (98.0%)	95.8% (91.7%)
R_{merge}	0.054 (0.439)	0.073 (0.484)	0.069 (0.523)
R,R_{free}	0.191,0.246	0.196,0.230	0.197,0.238
Number of atoms (protein, water)	962, 75	962, 57	964, 83
r.m.s.d. from bond ideality	0.008 Å	0.008 Å	0.009 Å
r.m.s.d. from angle ideality	1.57 °	1.52 °	1.49 °
Protein average B-factor	19.8 Å^2	23.64 Å^2	23.20 Å^2

studies (21), also pointed to a few glycines that were hinge points, which appeared to allow sub-structures in the protein to fluctuate with respect to each other. Interestingly, two of these glycines, Gly^{47} and Gly^{51}, fall within the PAS fold (22, 23) (see Fig. 1). PAS domains, originally identified in *Drosophila* clock proteins (24), have been found in a wide range of organisms (25). They have been shown to be involved in sensing of signals as part of signal transduction systems, as well as transcriptional activation (25). A recent study on the sequence similarities between PYP and PAS domains identified PYP as a possible prototype for the PAS fold (26). Most of the strongest sequence conservation is concentrated between residues 29 and 68 (22, 23, 26). This conservation is dominated by prolines and glycines (together ~6 residues out of 15 conserved residues). Thus, apart from their proposed role in the PYP photocycle (20), the conserved glycines could be important for the structure and/or conformational flexibility of the PAS domain.

Here, we investigate the role of the glycines at position 47 and 51 in the PYP photocycle and PAS domain function, using a multi-disciplinary approach. We describe the x-ray crystallographic structures and photocycle kinetics of the PYP mutants G47S, G51S, and G47S/G51S, which were designed to rigidify the mobile 48–53 region. The structures show no significant conformational changes, yet have significantly altered photocycle kinetics.

MATERIALS AND METHODS

Site-directed Mutagenesis, Purification, and Crystallization—The PYP variants PYP47, PYP51, and PYP47+51 were made by site-directed mutagenesis using the QuikChange site-directed mutagenesis procedure of Stratagene (Stratagene, Amsterdam, The Netherlands). The gene products were first screened using restriction analyses, and mutagenesis was subsequently confirmed by DNA sequencing. Recombinant His-tagged apoPYP and the three variants obtained through site-directed mutagenesis were produced heterologously in *Escherichia coli* and purified, as described previously (27). ApoPYP was reconstituted with *p*-coumaric acid as described previously (28). The obtained holo-PYP was used after removal of its polyhistidine tail.

PYP47, PYP51, and PYP47+51 crystallized under conditions similar to those reported previously (29). Freeze-dried protein was dissolved, passed over a gel filtration column in 50 mM phosphate buffer, pH 7, and concentrated to 25 mg/ml. Crystals were obtained by vapor diffusion experiments in which 1 μl of protein solution was mixed with an equal volume of well solution containing polyethylene glycol 2K monomethyl ether and 50 mM MES, pH 6.5. Crystals appeared within 3 days and grew as hexagonal rods, often with several rods joined at their bases. Larger and more regularly shaped crystals were obtained by microseeding.

Data Collection, Structure Solution, and Refinement—Diffraction data were collected on beamline X26C at the National Synchrotron Light Source, Brookhaven National Laboratory, using a 300 mm MAR Research image plate detector. Data were collected at 100 K by freezing crystals in an Oxford Cryosystems cryostream. See Table I for further details of the data collection statistics. Diffraction data were integrated and scaled with the HKL package (30).

The mutant structures were solved by molecular replacement using AMoRe (31) with PYP previously crystallized in $P6_5$ (PDB entry 2PHY (2)) as a search model, excluding the chromophore, with one molecule in the asymmetric unit. Using 8.0–4.0 Å data, a single solution was obtained for all mutants. After rigid body refinement in AMoRe, the R-factors were 0.337 (PYP47), 0.324 (PYP51), and 0.276 (PYP47+51), with correlation coefficients of 0.656 (PYP47), 0.723 (PYP51), and 0.786 (PYP47+51). Refinement was performed with CNS (32) with iterative model building using O (33). Details of the refinement can be found in Table I. After a few cycles of model building and placement of some well defined water molecules (4σ peaks in $|F_o|-|F_c|$, ϕ_{calc} maps and at least one hydrogen bond to the protein), the *p*-coumaric acid chromophore was well defined in the unbiased $|F_o|-|F_c|$, ϕ_{calc} maps and was built into the models. Further rounds of model building and refinement allowed placement of additional water molecules and assignment of some alternate side chain conformations, resulting in the final models (see Table I). Figures were prepared using Bobscript (34, 35), Raster3D (36), and GRASP (37).

Spectroscopy—UV/visual static- and transient-absorption spectra were recorded with a model 8453 Hewlett Packard diode array spectrophotometer (Portland, OR), which has a time resolution of 0.1 s. Typically UV/visible spectra from 250 to 550 nm were recorded every 0.1 s.

Laser-induced transient absorption spectroscopy (38) was carried out with a system composed of a Continuum Surelite I-10 YAG-laser (output intensity 140 mJ at 355 nm), a Continuum Surelite OPO (set at 446 nm), and a LP900 Spectrometer system, custom made by Edinburgh Analytical Instruments, Ltd. (Edinburgh, United Kingdom). The latter system contains a 450-Watt short-arc Xe lamp, in combination with a pulsed power supply and a Wright Instruments Peltier cooled CCD camera. The time resolution attainable with this set-up is 10 ns.

RESULTS

Crystal Structures—The crystal structures of PYP47, PYP51, and PYP47+51 were solved and refined to 1.75 Å, 1.85 Å, and 1.79 Å, respectively (Table I, Fig. 1). The structures were superimposed onto the wild type structure in the same crystal form ($P6_5$, WTPYP) (21) and compared. Table II lists the pairwise root mean square deviations (r.m.s.d.) of superposition of the mutant and wild type structures. In a previous study, the structures of native PYP crystallized in two different space groups ($P6_3$ *versus* $P6_5$) were compared, and it was found that the backbones superimposed with an r.m.s.d. of 0.5 Å (21). The crystal packing of the mutant structures (further discussed

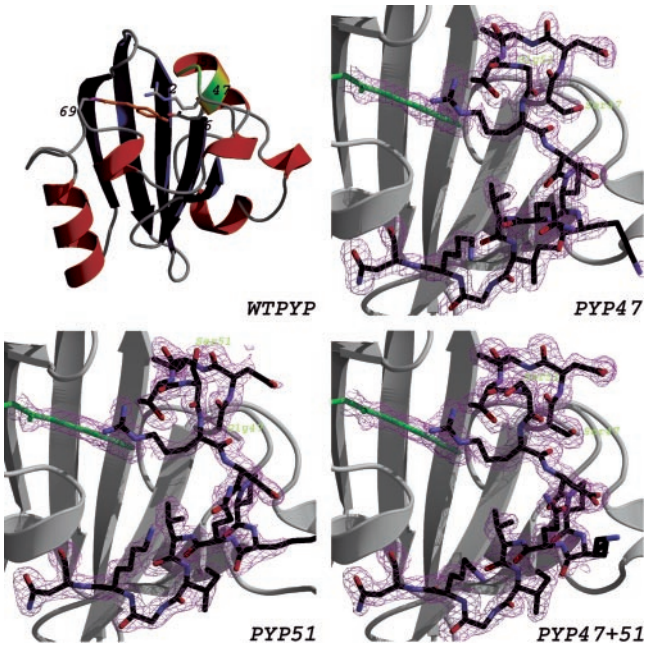

FIG. 1. **Overall PYP structure and electron density around the chromophore and the 47–61 region for PYP47, PYP51, and PYP47+51.** The WTPYP structure (21) is shown as a ribbon drawing colored by secondary structure. The key residues discussed in the paper are labeled, and the two positions of mutation (Gly^{47}/Gly^{51}) are further indicated by a *green patch*. In the mutant structures, the PYP backbone is shown as a *gray ribbon drawing*. The chromophore is shown as a *green sticks model*, all residues in the 47–61 regions are drawn with *black carbon atoms*. Residues 47/51 are identified with a label. The final $2|F_o|-|F_c|$, ϕ_{calc} maps (contoured at 1.25 σ) are shown in *magenta*.

TABLE II
Root mean squares deviation (Å) of the Cα positions after pairwise superposition

	WTPYP	PYP47	PYP51	PYP47 + 51
WTPYP				
PYP47	0.41			
PYP51	0.50	0.51		
PYP47 + 51	0.37	0.32	0.57	

below) is different in each case, as are the unit cell dimensions (Table I). Hence, the small differences observed in the backbones of the mutant structures are not significant, and the introduced mutations appear not to have affected the overall PYP structure. It seems that WTPYP, PYP47, and PYP47+51 show comparable r.m.s.d. to each other, but the r.m.s.d. of PYP51 superposition on these structures is >0.5 Å. Most of the differences are concentrated around residue 20, residue 52, and residue 100, as shown in Fig. 2. These regions were all involved in concerted motions as observed in the molecular dynamics simulations, crystal structures, and NMR structures (20, 21). The area around residue 20 is not well defined in the electron density maps. In previous PYP crystal structures, this area has high B-factors (2, 29), and in the NMR structure determination, this loop had too few restraints to accurately determine its conformation (39). Residues 47–61 (corresponding to the peak in Fig. 2) of the superimposed WTPYP and mutant structures are shown in Fig. 3. This region was well defined in the electron density maps of the mutants (Fig. 1). In WTPYP and all the mutants, the side chains of residues 47 and 51 are solvent-exposed and fit the local fold without steric hindrance. A serine at position 47 does make a (solvent-exposed) hydrogen bond, either to the backbone oxygen of residue 44 (in PYP47) or to the backbone oxygen of residue 52 (in PYP47+51). Ser^{51} in PYP51 and PYP47+51 does not interact with other residues. The 47–61 region makes different crystal contacts with symmetry-related residues, which accounts for the conformational changes observed for these residues. Although this region is almost fully solvent-exposed, only 1–3 hydrogen bonds to symmetry-related molecules are observed, for PYP47: Ile^{49}-Asn^{13}, Lys^{55}-Glu^{93}, and Gln^{56}-Glu^{74}; for PYP51: Asp^{48}-Lys^{64}, Thr^{50}-Lys^{17}, Gln^{56}-Gln^{22}, and Gly^{59}-Asn^{87}; for PYP47+51: Asp^{48}-Lys^{64} and Lys^{60}-Glu^{81}. In addition there are several water-mediated hydrogen bonds. The crystal contacts for WTPYP are essentially identical to those in PYP47+51.

For residues in the 47–61 range, some shifts in the backbone are observed, together with conformational changes in the side chains, due to the different crystal contacts for this region (see above). PYP47+51 is closer to the WTPYP structure in this area than either PYP47 and PYP51. This is in agreement with the relatively low r.m.s.d. in Table II. In PYP47+51 there are only three residues in this region with backbone shifts larger >0.4 Å (residues 54–56). For most of the 47–61 range, PYP47 stays close to the WTPYP conformation, except for residues 52–57, which show shifts in the backbone >0.4 Å, peaking at Pro^{54}. In PYP51 the conformational change is spread out over the 47–61 area, with residues 48–60 having backbone shifts >0.4 Å. The conformation of the 47–61 region can be compared in Figs. 3 and 4. The backbone ϕ,ψ angles of position 47 are in the α-helical region of the Ramachandran plot and barely change upon mutation to serine in either PYP47 or PYP47+51. Gly^{51} in WTPYP is with its ϕ,ψ angles (80° and 1°, respectively) in a disallowed region. Mutation to serine moves the torsion angles somewhat closer to the left-handed backbone region for PYP51, yet for the double mutant PYP47+51 they stay close to their WTPYP values (Fig. 4). It is thus likely that although the serine side chain appears to fit the local fold at residue 51, the backbone in PYP51 and PYP47+51 is likely to contain some strain as a result of the unfavorable ϕ,ψ angles.

Photocycle Kinetics—We have studied the effects of the mutations on the photocycle dynamics of PYP with transient absorption spectroscopy, using an experimental set-up described recently in detail elsewhere (38) that can reach a time-resolution of 10 ns. This allows investigation of the pR−pB and pB−pG transitions, which are on the μs and ms time scale, respectively. The results are summarized in Table III. For all three mutant proteins the pR−pB transition is faster than that in WTPYP. For PYP47 and PYP51 an ~2-fold increase is observed. There appears to be an additive effect in PYP47+51, where the rate increase (about 3-fold) is larger than that of either of the single mutations. On the other hand, the kinetics of the pB−pG transition shows a 3- to 4-fold rate decrease for PYP47 and PYP51. However, as is the case for the pR−pB transition, an additive effect is observed with the rate being 7-fold smaller for PYP47+51.

DISCUSSION

Previous analyses of protein conformational flexibility with computational techniques have indicated a key role for (conserved) glycine residues (40–43). Because of their unrestricted ϕ,ψ backbone torsion angles, they can act as pivotal points in the structure, allowing backbone segments to move relative to each other. In an earlier study toward the function of a conserved glycine in the cellular retinol-binding protein, it was found that mutation to a serine resulted in significantly altered retinol binding properties and inhibition of backbone motions (41, 44). In a similar study on thermolysin, mutation of conserved glycines involved in a hinge-bending motion resulted in a decrease in catalytic activity (40, 45). Hinge-bending glycines were also identified from a molecular dynamics simulation of PYP (20), supported by subsequent analysis of crystallographic and NMR structures (21). Computer simulations alone, how-

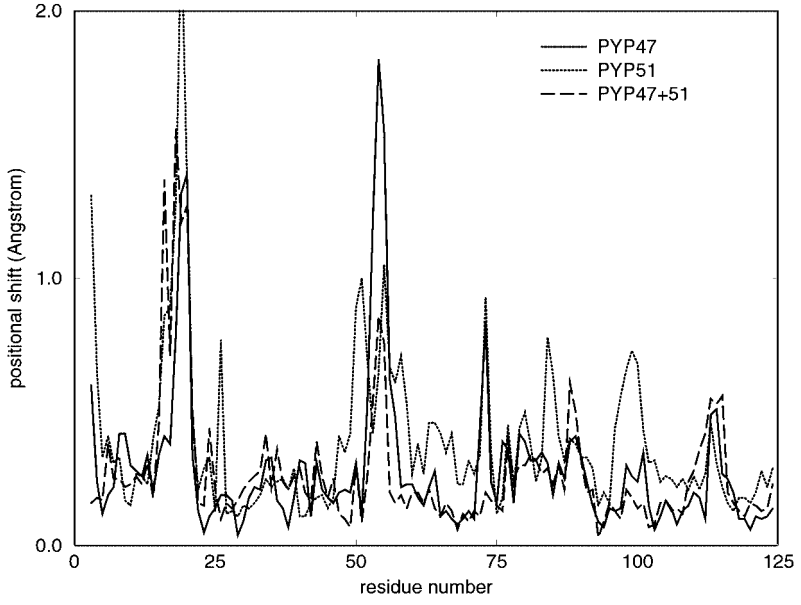

FIG. 2. **Positional shifts in PYP47, PYP51, and PYP47+51 compared with WTPYP.** Structures were superimposed on the Cα atoms (see also Table III) using WHAT IF (46). Positional shifts were then calculated for each mutant structure with respect to WTPYP.

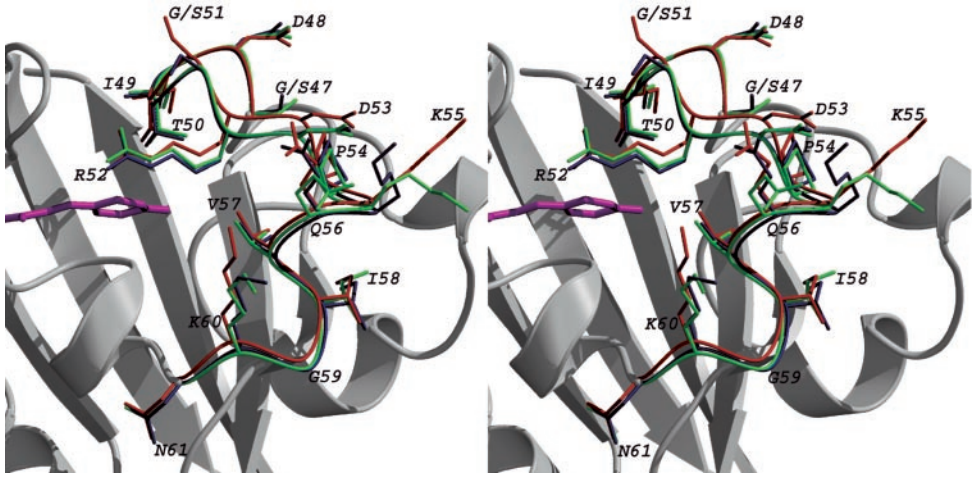

FIG. 3. **Conformational changes for residues 47–61.** The backbone of WTPYP is drawn in a *gray ribbon* representation with the chromophore drawn in a *magenta sticks representation*. For PYP47 (*green*), PYP51 (*red*), and PYP47+51 (*blue*), a Cα-trace and side chain atoms are shown for residues 47–61, which are further identified with labels.

ever, do not necessarily provide an accurate description of the real protein dynamics. They merely provide a model that can be tested experimentally. Here, we test the role of the proposed hinge-bending glycine residues by mutagenesis together with spectroscopic analyses and by direct comparison of the simulated dynamics with the conformational changes seen in the experimental structures.

Glycines 47 and 51 are located in a region of the protein that is close to the chromophore and is known to be mobile in the crystal structures (2). This region is also mobile in computer simulations (20, 21), with the short helices α3 and α4 showing a hinge-bending motion with respect to each other and the chromophore. The Cα atoms of both glycines are solvent-exposed. A mutation to serine would result in a conformationally restricted backbone, while not significantly altering the local structure. If these mutations indeed rigidify the local backbone and if the flexibility of this area is an important aspect of PYP dynamics, significant effects on the spectroscopically measured photocycle kinetics should be observed with a clear additive component in a mutant with both Gly−Ser substitutions.

Some small conformational changes were observed in the structures of PYP47, PYP51, and PYP47+51, compared with WTPYP, which are due to the different crystal packing contacts in the 47–61 region. In the context of these altered crystal contacts, the conformational change for PYP47 is noteworthy, as the backbone immediately surrounding the mutation itself is hardly altered (Figs. 3 and 4), yet a shift is observed around residue 54. The serine substitution at position 51 results in a small change of backbone conformation for this residue (Fig. 4), producing some conformational change of the neighboring backbone (Figs. 3 and 4). The double mutation, however, results in a conformation relatively close to WTPYP (and has the same crystal contacts as WTPYP).

The spectroscopic data show that the mutations have indeed affected the dynamics of the protein (Table III). Although the pB-pG transition is slowed down with a clear additive effect for the PYP47+51 double mutant, the pR-pB transition appears to occur faster in the mutants than in native PYP (also with an additive effect). If the backbone segment around the mutations is rigidified, one would expect the pR−pB and pB−pG transitions both to be slower. The faster pR−pB transition may be due to strain in the backbone, introduced by the mutations. This can be understood by inspection of the Ramachandran plots, which show that introduction of a serine instead of a glycine at position 51 results in unfavorable backbone torsion angles (Fig. 4). The strain thus introduced in the backbone may

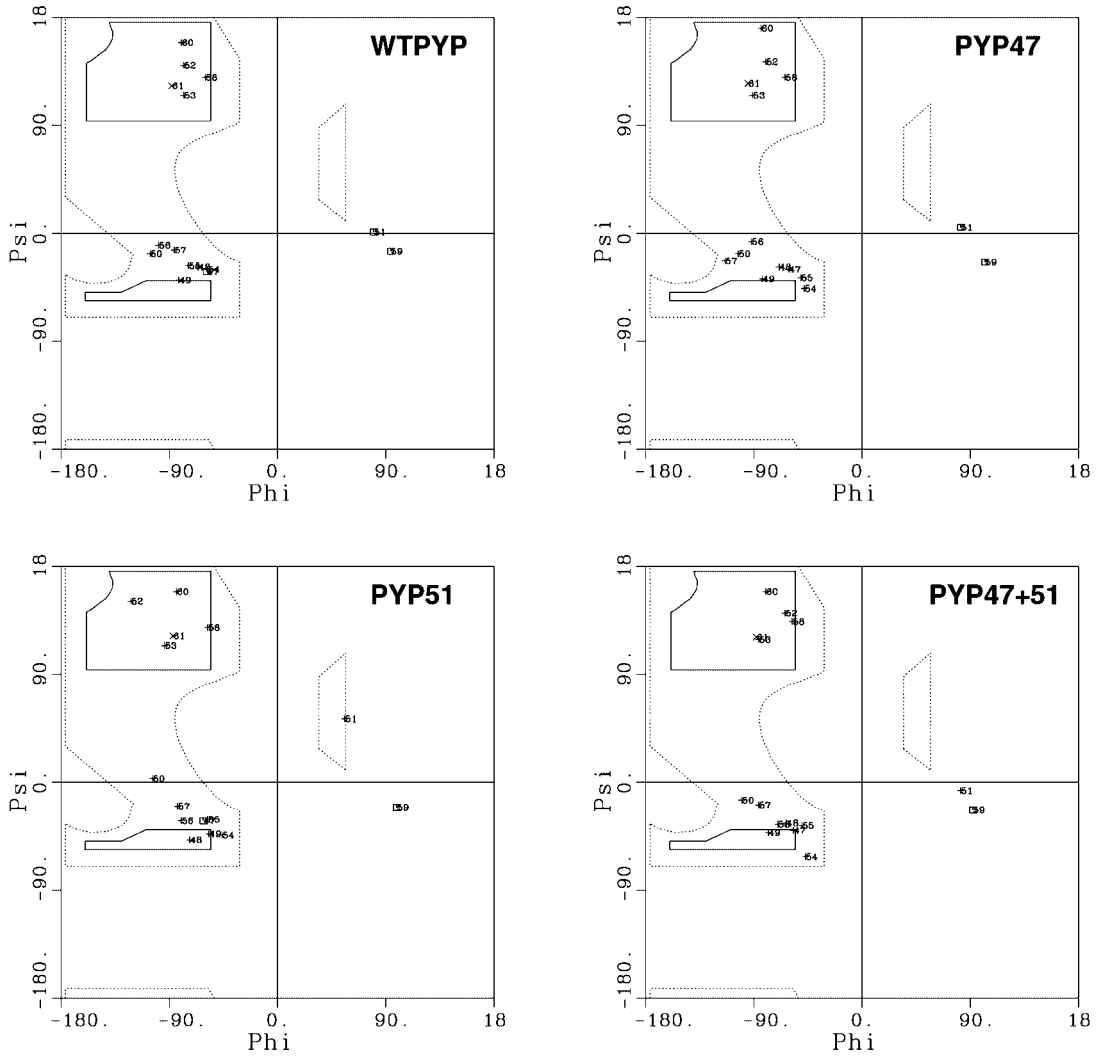

FIG. 4. **Ramachandran plots of residues 47–61 in WTPYP and mutant structures.**

TABLE III
Photocycle kinetics of WTPYP and mutants

	WTPYP	PYP47	PYP51	PYP47 + 51
pR-pB (μs)	448	193	252	159
pB-pG (ms)	131	504	368	858

be released in the pR-pB transition (when the protein is known to undergo a major conformational change (17–20), thereby lowering the free energy of this transition in the mutant structures compared with the native structure.

One of the glycines studied here, Gly^{51}, is part of the sequence signature of the PAS domains, of which PYP was proposed to be a structural prototype (26). Arg^{52}, next to Gly^{51} in PYP, is in contact with the chromophore and has been shown to change position in the later stages of the photocycle (4). In many other PAS domains, this Arg^{52} is substituted for a tyrosine, which is proposed to point into a binding pocket (26). In analogy to what we observe here for PYP, we propose that a flexible Gly^{51} may also play a key role in PAS domain dynamics, which would then suggest that in all these structurally similar signal transduction modules, biological activity is mediated via the conserved intrinsic functional dynamical properties.

Acknowledgment—We gratefully acknowledge Ivo van Stokkum for his expert assistance in analyzing the initial spectroscopic data.

REFERENCES

1. Sprenger, W. W., Hoff, W. D., Armitage, J. P., and Hellingwerf, K. J. (1993) *J. Bacteriol.*, **175,** 3096–3104
2. Borgstahl, G. E. O., Williams, D. R., and Getzoff, E. D., (1995) *Biochemistry* **34,** 6278–6287
3. Xie, A. H., Hoff, W. D., Kroon, A. R., and Hellingwerf, K. J. (1996) *Biochemistry*, **35,** 14671–14678
4. Perman, B., Srajer, V., Ren, Z., Teng, T., Pradervand, C., Ursby, T., Bourgeois, D., Schotte, F., Wulff, M., Kort, R., Hellingwerf, K., and Moffat, K. (1998) *Science*, **279,** 1946–1950
5. Kort, R., Vonk, H., Xu, X., Hoff, W. D., Crielaard, W., and Hellingwerf, K. J. (1996) *FEBS Lett.*, **32,** 73–78
6. Genick, U. K., Borgstahl, G. E. O., Kingman, N., Ren, Z., Pradervand, C., Burke, P. M., Srajer, V., Teng, T., Schildkamp, W., McRee, D. E., Moffat, K., and Getzoff, E. D. (1997) *Science*, **275,** 1471–1475
7. Genick, U. K., Soltis, S. M., Kuhn, P., Canestrelli, I. L., and Getzoff, E. D. (1998) *Nature* **392,** 206–209
8. Baltuska, A., van Stokkum, I. H. M., Kroon, A., Monshouwer, R., Hellingwerf, K. J., and van Grondelle, R. (1997) *Chem. Phys. Lett.* **270,** 263–266
9. Changenet, P., Zhang, H. (1998) *Chem. Phys. Lett.* **282,** 276–282
10. Meyer, T. E., Tollin, G., Causgrove, T. P., Cheng, P., and Blankenship, R. E. (1991) *Biophys. J.*, **59,** 988–991
11. Chosrowjan, H.,Mataga, N., Nakashima, N., Imamoto, Y., and Tokunaga, F., (1997) *Chem. Phys. Lett.*, **270,** 267–272
12. Ujj, L., Devanathan, S., Meyer, T. E., Cusanovich, M. A., Tollin, G., and Atkinson, G. H. (1998) *Biophys. J.* **75,** 406–412
13. Hoff, W. D., van Stokkum, I. H. M., van Ramesdonk, H. J., van Brederode, M. E., Brouwer, A. M., Fitch, J. C., Meyer, T. E., van Grondelle, R., and Hellingwerf, K. J. (1994) *Biophys. J.*, **67,** 1691–1705
14. Meyer, T. E., Yakali, E., Cusanovich, M. A., and Tollin, G. (1987) *Biochemistry*, **26,** 418–423
15. Hoff, W. D., Kwa, S. L. S., van Grondelle, R., and Hellingwerf, K. J. (1992) *Photochem. Photobiol.*, **56,** 529–539
16. Miller, A., Leigeber, H., Hoff, W. D., and Hellingwerf, K. J. (1998) *Biochim. Biophys. Acta*, **1141,** 190–196
17. van Brederode, M. E., Hoff, W. D., van Stokkum, I. H. M., Groot, M. L., and

Hellingwerf, K. J. (1996) *Biophys. J.*, **71,** 365–380
18. Rubinstenn, G., Vuister, G. W., Mulder, F. A. A., Dux, P. E., Boelens, R., Hellingwerf, K. J., and Kaptein, R. (1998) *Nat. Struct. Biol.*, **5,** 568–570
19. Hoff, W. D., Xie, A., van Stokkum, I. H. M., Tang, X.-J., Gural, J., Kroon, A. R., and Hellingwerf, K. J. (1999) *Biochemistry*, **38,** 1009–1017
20. van Aalten, D. M. F., Hoff, W. D., Findlay, J. B. C., and Crielaard, W., Hellingwerf, K. J. (1998) *Protein Eng.*, **11,** 873–879
21. van Aalten, D. M. F., Crielaard, W., Hellingwerf, K. J., and Joshua-Tor, L. (2000) *Protein Sci.*, **9,** 64–72
22. Lagarias, D. M., Wu, S.-H., and Lagarias, J. C. (1995) *Plant Mol. Biol.* **29,** 1127–1142
23. Crosthwaite, S. K., Dunlap, J. C., and Loros, J. J. *Science*, (1997) **276,** 763–769
24. Nambu, J. R., Lewis, J. O., Wharton, K. A., and Crews, S. T. (1991) *Cell*, **67,** 1157–1167
25. Zhulin, I. B., and Taylor, B. L. (1997) *Trends Biochem. Sci.*, **22,** 331–333
26. Pellequer, J.-L., Wager-Smith, K. A., Kay, S. A., and Getzoff, E. D. (1998) *Proc. Natl. Acad. Sci. U. S. A.*, **95,** 5884–5890
27. Kort, R., Hoff, W. D., van West, M., Kroon, A. R., Hoffer, S. M., Vlieg, K. H., Crielaard, W., van Beeumen, J. J., and Hellingwerf, K. J. (1996) *EMBO J.*, **15,** 3209–3218
28. Kroon, A. R., Hoff, W. D., Fennema, H. P. M., Gijzen, J., Koomen, G.-J., J. W. Verhoeven, J. W., Crielaard, W., and Hellingwerf, K. J. (1996) *J. Biol. Chem.*, **271,** 31949–31956
29. van Aalten, D. M. F., Crielaard, W., Hellingwerf, K. J., and Joshua-Tor, L. (2001)**,** *Acta Crystallogr.,* in press
30. Otwinowski, Z., and Minor, W. (1997) *Meth. Enzymol.* **276,** 307–326
31. Navaza, J. (1994) *Acta Crystallogr.,* **A50**, 157–163
32. Brunger, A. T., Adams, P. D., Clore, G. M., Gros, P., Grosse-Kunstleve, R. W., Jiang, J.-S., Kuszewski, J., Nilges, M., Pannu, N. S., Read, R. J., Rice, L. M., Simonson, T., and Warren, G. L. *Acta Crystallog.* (1998) **D54**, 905–921
33. Jones, T. A., Zou, J. Y., Cowan, S. W., and Kjeldgaard, M.(1991) *Acta Crystallog.,* **A47**, 110–119
34. Kraulis, P. J. (1991) *J. Appl. Crystallog.*, **24,** 946–950
35. Esnouf, R. M. (1997) *J. Mol. Graph.*, **15,** 132–134
36. Merritt, E. A., and Murphy, M. E. P. (1994) *Acta Crystallogr.,* **D50,** 869–873
37. Nicholls, A., Sharp, K., and Honig, B. (1991) *Proteins*, **11,** 281–296
38. Hendriks, J., Hoff, W. D., Crielaard, W., and Hellingwerf, K. J. (1999) *J. Biol. Chem.*, **274,** 17655–17660
39. Dux, P., Rubinstenn, G., Vuister, G. W., Boelens, R., Mulder, F. A. A., Hard, K.,Hoff, W. D., Kroon, A., Crielaard, W., Hellingwerf, K. J., and Kaptein, R. (1998) *Biochemistry*, **37,** 12689–12699
40. van Aalten, D. M. F., Amadei, A., Linssen, A. B. M., Eijsink, V. G. H.,Vriend, G., and Berendsen, H. J. C. (1995) *Proteins*, **22,** 45–54
41. van Aalten, D. M. F., Findlay, J. B. C., Amadei, A., Berendsen, and H. J. C. (1995) *Protein. Eng.*, **8,** 1129–1135
42. Mello, L. V., van Aalten, D. M. F., and Findlay, J. B. C. (1997) *Protein. Eng.*, **10,** 381–387
43. Mello, L. V., van Aalten, D. M. F., and Findlay, J. B. C. (1998) *Biochemistry* **37,** 3137–3142
44. van Aalten, D. M. F. Jones, P. C., de Sousa, M., and Findlay, J. B. C. (1997) *Prot. Eng.*, **10,** 31–37
45. Veltman, O. R., Eijsink, V. G. H., Vriend, G., de Kreij, A., Venema, G., and van den Burg, B. (1998) *Biochemistry*, **37,** 5305
46. Vriend, G.,(1990) *J. Mol. Graph.*, **8,** 52–56